



# Design and synthesis of imine linked ZnO nanoparticles functionalized with Al(III), candidate for application in light emitting diodes

Charu Madhu<sup>1</sup> · Inderpreet Kaur<sup>2</sup> · Navneet Kaur<sup>3</sup>

Received: 22 November 2017 / Accepted: 14 February 2018 / Published online: 19 February 2018  
© Springer Science+Business Media, LLC, part of Springer Nature 2018

## Abstract

Zinc oxide nanoparticles **1.ZnO** decorated with dipodal organic receptor **1** bearing imine linkage were synthesized using wet chemical precipitation technique. The imine linked receptor **1** used as capping agent was synthesized using condensation reaction. **1.ZnO** nanoparticles were characterized through FTIR, SEM, TEM, DLS and fluorescence spectroscopy. The emission spectra of surface modified ZnO nanoparticles authenticated the passivation of surface defects and dangling bonds which otherwise are available on the surface of uncapped ZnO nanoparticles. **1.ZnO** nanoparticles demonstrated blue emission at 461 nm. The binding affinity of **1.ZnO** nanoparticles was also checked in presence of metal ions through changes observed in the emission spectra. An enhancement up to threefold in the fluorescence intensity was achieved from **1.ZnO** nanoparticles upon coordination with Al<sup>3+</sup> metal ion. The results demonstrated that our design strategy resulted in pure and narrow emission with FWHM 70 nm. This effective way of achieving the selectivity factor and enhanced quantum yield can be utilized in electronic device like light emitting diodes.

## 1 Introduction

Nanoparticles with size < 100 nm possess unique optoelectronic properties in comparison to their bulk counterpart. The unique properties of nanomaterials led to their use in electronic devices [1–3]. The use of nanotechnology in electronics to reduce the device size is one option for the continuous progress in silicon industry which requires tradeoff between the device performance and power consumption [4], the other option is the use of nanomaterials such as quantum dots as new materials that can replace

the conventional materials [5, 6]. A variety of nanomaterials are being used for number of electronic applications like lasers, lighting technologies, semiconductor chips, fuel cells, lithium ion batteries, solar cells and so on. The nanomaterials selected for specific device application should be biodegradable, safe, non-toxic and should also result in low cost electronics. The biodegradable and non toxic nanoparticles are favored for their impending applicability in targeted drug delivery and in biophotonic devices [7, 8]. Due to copious applications, studies on the synthesis, characterization and properties of nanoparticles have received significant attention in the past several years. Among the semiconductor nanoparticles like ZnO, TiO<sub>2</sub>, SnO<sub>2</sub>, wurtzite n-type semiconductor zinc oxide nanoparticles have got a lot of attention in research community because of their unique properties. ZnO can be employed for the fabrication of optoelectronic nanodevices for its direct wide band gap (3.37 eV) and high exciton binding energy (60 meV) at room temperature, nearly 2.4 times that of GaN, for its outstanding structural and physical properties, for it is relatively abundant, chemically stable, easy to synthesize and of course non-toxic [9]. The large exciton binding energy makes it possible to employ excitonic recombination process as a lasing mechanism at lower threshold voltage and thus, ZnO is a striking applicant for technological applications [10]. Furthermore,

**Electronic supplementary material** The online version of this article (<https://doi.org/10.1007/s10854-018-8776-y>) contains supplementary material, which is available to authorized users.

✉ Charu Madhu  
charu\_uiet@pu.ac.in

✉ Navneet Kaur  
navneetkaur@pu.ac.in

<sup>1</sup> University Institute of Engineering and Technology (UIET), Panjab University, Chandigarh 160014, India

<sup>2</sup> Biomolecular Electronics and Nanotechnology Division (BEND), Central Scientific Instruments Organization (CSIO), Chandigarh 160030, India

<sup>3</sup> Department of Chemistry, Panjab University, Chandigarh 160014, India

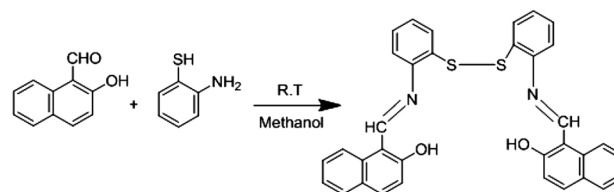
ZnO has higher electron mobility and the corresponding electron diffusion coefficient in comparison to TiO<sub>2</sub>. ZnO is widely used in dye sensitized solar cells, lasers, light emitting diodes (LED), as a transparent conducting oxide, touch panels and memory devices, gas sensors, photocatalysts and photodetectors [11, 12]. ZnO can be synthesized by different chemical and physical methods like hydrothermal method, sol–gel, vapor condensation, laser ablation, mechanical milling, microemulsion techniques, microwave method etc. However, in most of these techniques, nanoparticles tend to agglomerate due to their high surface energy [13]. The chemical synthesis technique is the low cost and simplest one to synthesize ZnO nanoparticles where morphology of nanoparticles can be controlled by optimizing concentration of precursors, temperature and reaction time [14]. The fluorescence spectrum of intrinsic ZnO nanoparticles show emission in UV region due to excitonic transitions and broad emission in visible region due to deep level transitions [15] and it is also cited in the literature that the intensity of emission in the UV range for uncapped ZnO nanoparticles is less than the intensity of emission in visible region which is owed to the presence of many surface defects viz. zinc interstitial, oxygen vacancies, zinc vacancies and a number of acceptor and donor pairs [16]. The presence of these defects set up different electronic levels within the band gap that are responsible for the nonradiative recombination of the photo generated electrons and hole pairs, which result in transitions by these levels [9, 17, 18]. To improve the efficiency of UV devices, it is essential to inhibit the defect related green emission in the visible region of spectrum. As the size of nanoparticle reduces, the increased S/V ratio results in increase in surface defects, and that too is responsible for the agglomeration of nanoparticles. The agglomeration can be avoided if the growth of nanoparticle can be stopped immediately after the nucleation stage, by the use of capping agent (CA). The capping monolayer of an organic receptor is used to help stabilization of nanoparticles and thus prevents the ZnO nanoparticles from aggregation [19–22]. The coating of ZnO nanoparticles with the receptors also result in static conformal geometry as the free rotation of the ligand would be restricted, leading to increase in the selectivity of nanoparticles. The surface modification of nanoparticles also showed improvement in both PL intensity and EL efficiency [23]. In the present work, ZnO nanoparticles are synthesized by wet chemical precipitation route with the involvement of CAs to modify the surface defects. The research work is focused on the transformation of photophysical properties of nanostructured ZnO semiconductors that lead to the variation in the band gap. In continuation to the research interest of our group [24–27], the imine linked dipodal organic receptor is used to decorate the surface of ZnO nanoparticles,

which demonstrated improvement in optoelectronic properties of capped ZnO nanoparticles and increase in the selectivity too.

## 2 Experiment details

### 2.1 Materials and methods

Zinc nitrate hexahydrate, sodium hydroxide, 2-hydroxy-1-naphthaldehyde, 2-aminothiophenol, were all purchased from Sigma Aldrich and were used without further purification. <sup>1</sup>H NMR spectra of organic receptor **1** and **1.ZnO** were obtained from JNM-ECS400 (JEOL) NMR spectrophotometer at 400 MHz. An Agilent 7700 Series ICP-mass spectrometer was used for the determination of the mass of the compounds. The ICP–MS instrument was equipped with an ASX-500 series ICP–MS auto-sampler. The elemental and morphology analysis was carried out with scanning electron microscope (SEM JEOL JSM-6610LV) at 15 kV voltage. TEM images were recorded on Hitachi instrument (H-7500) at 100 kV. For TEM measurements the organic receptor coated ZnO nanoparticles were dispersed homogeneously in methanol solvent using ultrasonic treatment. A tiny drop of this solution was directed on to a carbon-coated copper grid followed by subsequently drying in air before transfer it in to microscope. The particle size was determined using dynamic light scattering (DLS), with the external probe feature of a MetrohmMicrotrac Ultra Nanotracer Particle Size Analyzer. FTIR spectrophotometer Thermo Fisher Scientific Inc., USA was used to confirm the functional groups of organic receptor and to observe shift in the bands in case of surface modified ZnO nanoparticles. The sample used for this measurement was in the form of pellets prepared by mixing 1% weight of nanoparticles with KBr. Perkin Elmer LS55 Fluorescence spectrophotometer was used to carry out the fluorescence measurements. DFT calculations were performed on Gaussian 03 program by using B3LYP/6-311G basis set.



**Scheme 1** Synthesis of organic receptor **1**

## 2.2 Synthesis of organic receptor and surface passivated ZnO nanoparticles

The organic receptor **1** was synthesized by condensation reaction between 2-hydroxy-1-naphthaldehyde (1.72 gm, 10 mM) and 2-aminothiophenol (1.07 ml, 10 mM) in dry methanol (30 ml) under O<sub>2</sub> and basic conditions (Scheme 1). After completion of reaction, the precipitates were filtered and washed with methanol several times to get rid of impurities. The resultant yellow solid fine particles were dried for 40 h. ZnO nanoparticles were synthesized by taking an alcoholic solution of zinc nitrate hexahydrate (1.796 mM, 0.5335 g) along with organic receptor (3.593 mM, 2 g) in round bottom flask. The reaction was kept on continuous stirring at room temperature. Alcoholic solution of sodium hydroxide (2.695 mM, 0.1078 g) was then added drop by drop.

The stirring of the solution was kept continuous for 4 h and a dispersion of ZnO nanoparticles was formed gradually in the solution. The as prepared dispersion of ZnO nanoparticles was filtered and washed with methanol

and water several times. The resultant fine nanoparticles were then dried for 72 h. The ligand was characterized by <sup>1</sup>H NMR (Fig. S1). <sup>1</sup>H NMR (400 MHz, DMSO-*d*<sub>6</sub> ppm) δ: 7.14 (d, 2H, ArH), 7.25 (t, 2H, ArH), 7.38 (m, 4H, ArH), 7.58 (t, 2H, ArH), 7.60 (d, 2H, ArH), 7.70 (d, 2H, ArH), 7.85 (d, 2H, ArH), 7.9 (d, 2H, ArH), 8.5 (d, 2H, ArH), 9.6 (s, 2H, -CH=N). Ligand was also characterized by mass spectroscopic technique ESI-MS, which shows *m/z* = 557.3 [M+H]<sup>+</sup>, where M = C<sub>36</sub>H<sub>28</sub>N<sub>2</sub>O<sub>2</sub>S<sub>2</sub> (Fig. S2) and DFT calculations were performed using Gauss View 03 software. DFT calculations were made to realize the optimized structure of the organic receptor (Fig. S1). The optimized structure has band gap of 3.48 eV (Fig. S3).

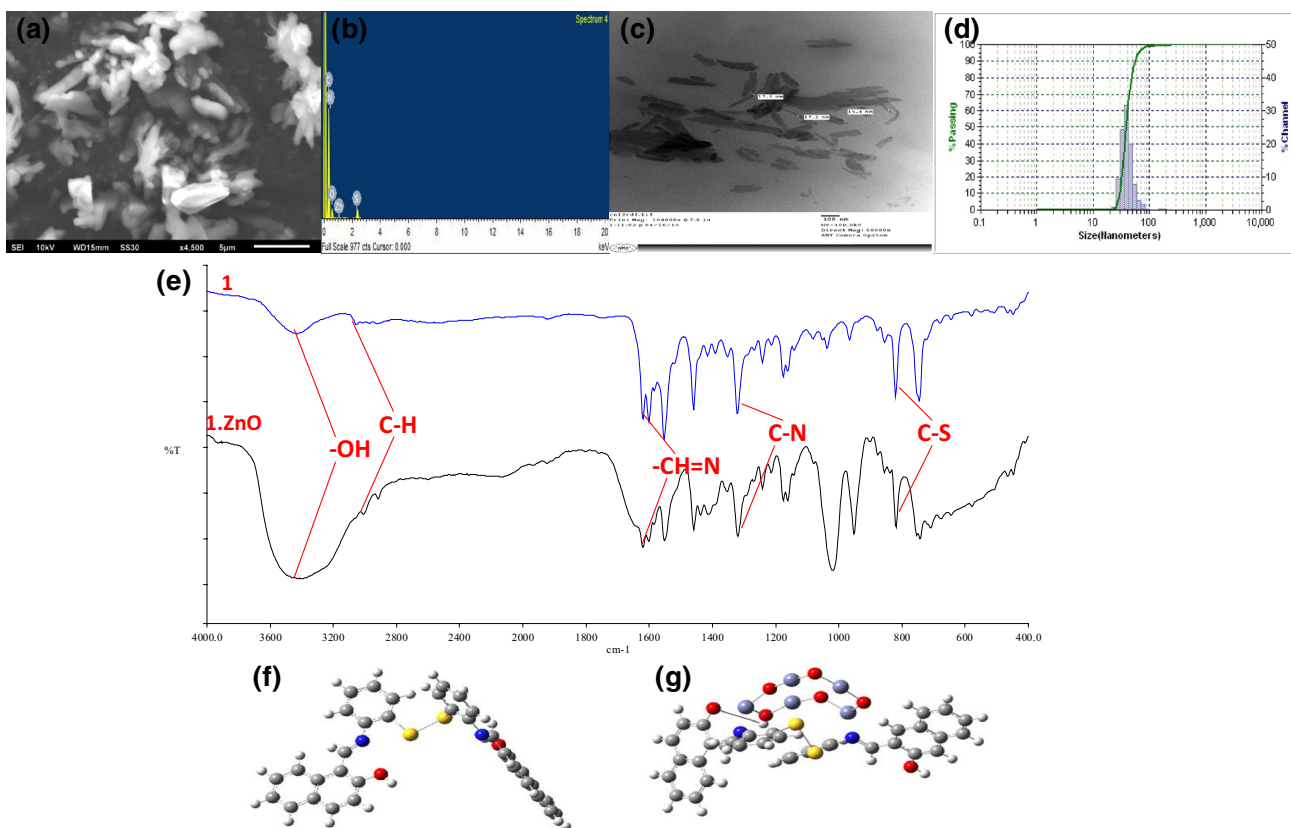


**Fig. 1** **a** SEM image of **1.ZnO** showing grain like structure. **b** EDX analysis of **1. ZnO** showing the existence of organic compound together with ZnO. **c** TEM image of **1.ZnO** showing size 17 nm. **d** DLS based particle size analyzer showing particle size of 30 nm. **e** A

comparison of FTIR spectrum of organic receptor (above) and ZnO capped with organic receptor (below). **f** DFT optimized geometry of organic compound **1**. **g** Optimized geometry of organic receptor capped ZnO nanoparticles **1.ZnO**

### 3 Results and discussion

#### 3.1 Characterization of surface passivated ZnO nanoparticles

Organic receptor **1** was used as a capping monolayer over the surface of ZnO nanoparticles in order to get rid of the surface defects whose influence increases with reduction in the size of ZnO nanoparticles. The morphology of the ZnO nanoparticles was realized using scanning electron microscopy (SEM). The SEM image demonstrated the grain like structure of synthesized ZnO nanoparticles (Fig. 1a) It is very well cited in literature that the presence of CAs direct the growth of nanoparticles in a rigorous direction [28, 29]. **1.ZnO** nanoparticles have demonstrated self assembled structure due to the presence of structure directing agent **1**. The organic receptor **1** may get attached to the surface of ZnO nanoparticles through –SH, –NH or –OH bond thereby controlling the morphology of particles by preventing aggregation. The elemental analysis was done using energy dispersive X-ray spectrum (EDX), which confirmed the coating of organic receptor over the surface of ZnO nanoparticles (Fig. 1b). The image demonstrated the presence of elements C, N of organic compound along with Zn and O. TEM image of **1.ZnO** is showing that its several units are assembled together to form a bigger particle size (Fig. 1c). This can be due to intermolecular hydrogen bonding between –CH=N– of **1** and –OH group of ZnO.

The distribution of particle size of organic ligand directed ZnO nanoparticles **1.ZnO**, showing average particle size of 30 nm, was measured with DLS based particle size analyzer (Fig. 1d) by dissolving the compound in DMSO:H<sub>2</sub>O (70:30; v/v). DLS was showing somewhat larger particle size as compared to TEM analysis due to hydro-dynamic radius of nano-aggregates formed during DLS analysis. The structural analysis of surface passivated ZnO nanoparticles was also supported through the IR spectrum, where a series of peaks were observed from 400 to 4000 cm<sup>-1</sup> (Fig. 1e). Shifts observed in respective peaks of functional groups in IR spectra of surface decorated ZnO nanoparticles in comparison to that of organic receptor demonstrate the influence of CA [30]. The IR spectra demonstrated the absorption bands corresponding to the functional groups of **1** and **1.ZnO**. The exact nature of binding site of **1** responsible for coordination with ZnO was determined from changes in the IR spectrum of **1** upon interaction with ZnO. The IR spectra demonstrated the broadness in peaks observed at 3430 and 1621 cm<sup>-1</sup>, which corresponds to the stretching vibration of –OH group and (–CH=N–) group of organic receptor **1** upon its interaction with ZnO. Peak at 1020 cm<sup>-1</sup> confirmed to the bending

vibrations of =C–H bond. The peak at 1320 cm<sup>-1</sup> is due to C–N stretching absorption for aromatic amines which remains intact in case of **1** and **1.ZnO**. DFT calculations were also run to observe the interaction of **1** with ZnO nanoparticles (Fig. 1g). The optimized geometry of **1** and **1.ZnO** is compared. The optimized geometry of dipodal receptor used as CA had both arms perpendicular to each other in the absence of ZnO nanoparticles represented by a small cluster (ZnO)<sub>5</sub>. A clear change in the bond length of –OH group of **1** was observed when dipodal receptor was taken in environment of ZnO nanoparticles. Moreover, the optimized geometry clearly demonstrated the development of a fix cavity between the two arms closer to the disulphide bond. It can be inferred that the interaction of organic receptor with the surface of ZnO nanoparticles has resulted in static conformal geometry as the free rotation of the ligand would have restricted, which ultimately led to the increase in the selectivity of nanoparticles.

The HOMO densities are now completely concentrated on (ZnO)<sub>5</sub> cluster with LUMO densities symmetrically concentrated on the disulphide bond of 2-aminothiophenol ring (Fig. S3). The energy of optimization also proved that the optimized geometry of ZnO nanoparticles capped with an organic receptor was more stable than that of organic receptor and ZnO nanoparticles separately (Table 1).

#### 3.2 Photoluminescence studies of surface passivated ZnO nanoparticles

The photoluminescence spectra of pure ZnO nanoparticles have two types of emissions: the emission in the visible region due to the deep level transitions and the emission in the UV region due to the excitonic transitions. The deep level transitions are due to the surface defects present in pure ZnO nanoparticles, the intensity of which also increases as the size of nanoparticle reduces [31]. The capping layer of organic receptor over ZnO nanoparticle surface stops the growth of ZnO nanoparticles immediately soon the nucleation stage [32]. So, the size of ZnO nanoparticles may get controlled. The CA protects the ZnO nanoparticles from aggregation, and thus may reduce the surface defects. Finally, the optoelectronic properties may get improved if the surface related visible emission could get censured. The PL spectra of pure ZnO exhibited a green emission band

**Table 1** The optimization parameters of ZnO, organic receptor, ZnO with organic receptor calculated at B3LYP/6-311G level

	Energy (a.u.)
ZnO	– 9272.73 a.u.
Organic receptor <b>1</b>	– 2366.3 a.u.
ZnO with organic receptor	– 11639.3 a.u.

at 570 nm [33, 34]; however this band gets quenched upon capping of ZnO with **1**. This noticed effect is very well elucidated in literature [35]. According to Dijken et al. the reason for the occurrence of multiple emission peaks in visible region in case of uncapped ZnO is the formation of recombination centre ( $\text{Vo}^{**}$ ), where the valence band hole is trapped by the surface state and then tunnels back into oxygen vacancies containing one electron ( $\text{Vo}^*$ ). This recombination of a shallow trapped electron with a deeply trapped hole in a  $\text{Vo}^{**}$  center is responsible for visible emission. The PL emission spectrum of **1.ZnO** nanoparticles excited at 341 nm showed a sharp emission peak at 461 nm with a shoulder at 380 nm. The observed band at 380 nm is assigned to the excitonic emission from ZnO nanoparticles and 461 nm in case of **1.ZnO** is due to the association of organic receptor **1** with ZnO. Similar type of emission band at 420 nm was also observed in the fluorescence spectra of receptor **1** indicating that the observed band for **1.ZnO** is due to the emission from imine linkage. For the use of ZnO nanoparticles in devices like LEDs, the selectivity factor is important. The broad emission in the visible range owing to the presence of surface defects may result in the white light by combination of all the emitted colors from pure ZnO nanoparticles [36]. However, if the specific color is desired, the broad emission in the visible region needs to be improved. The capping layer of organic receptor **1** used to decorate the surface of ZnO

nanoparticles, limit the defect originated emission. Figure 2a shows the room temperature PL spectra with emission at 461 nm from surface improved ZnO nanoparticles. Clearly the figure shows that the defect related emission and dangling bonds available at the surface of uncapped ZnO nanoparticles is reduced and also the selectivity factor is achieved as the **1.ZnO** nanoparticles resulted in blue emission at only 461 nm. Dijken et al. [35] also presented a model where it was showed that capping of the metal oxide semiconductor nanoparticles resulted in passivation of surface defects. From the existing literature, it is observed that the organic receptors are good CAs for metal oxide nanoparticles, as they can nicely passivate the surface defects and thus lessens the defect related visible emission [37]. In order to check the binding affinity of **1.ZnO** nanoparticles, change in the emission profile of ZnO nanoparticles is practiced upon addition of a particular metal nitrate salt as the photophysical properties of the fluorescent chemosensors changes upon its interaction with the chemical species in such a way that its fluorescent signatures are observed [38].

All the recognition studies were carried out at  $25 \pm 1^\circ\text{C}$ , and before recording any spectrum, sufficient time was given for shaking to ensure the uniformity of the solution. of the presence of different cations, including  $\text{Li}^+$ ,  $\text{Na}^+$ ,  $\text{K}^+$ ,  $\text{Mg}^{2+}$ ,  $\text{Ca}^{2+}$ ,  $\text{Sr}^{2+}$ ,  $\text{Ba}^{3+}$ ,  $\text{Cr}^{3+}$ ,  $\text{Mn}^{2+}$ ,  $\text{Co}^{2+}$ ,  $\text{Zn}^{2+}$ ,  $\text{Ag}^+$ ,  $\text{Cd}^{2+}$ ,  $\text{Hg}^{2+}$ ,  $\text{Pb}^{2+}$ ,  $\text{Cs}^{2+}$  and  $\text{Al}^{3+}$  (Fig. 2b). The metal

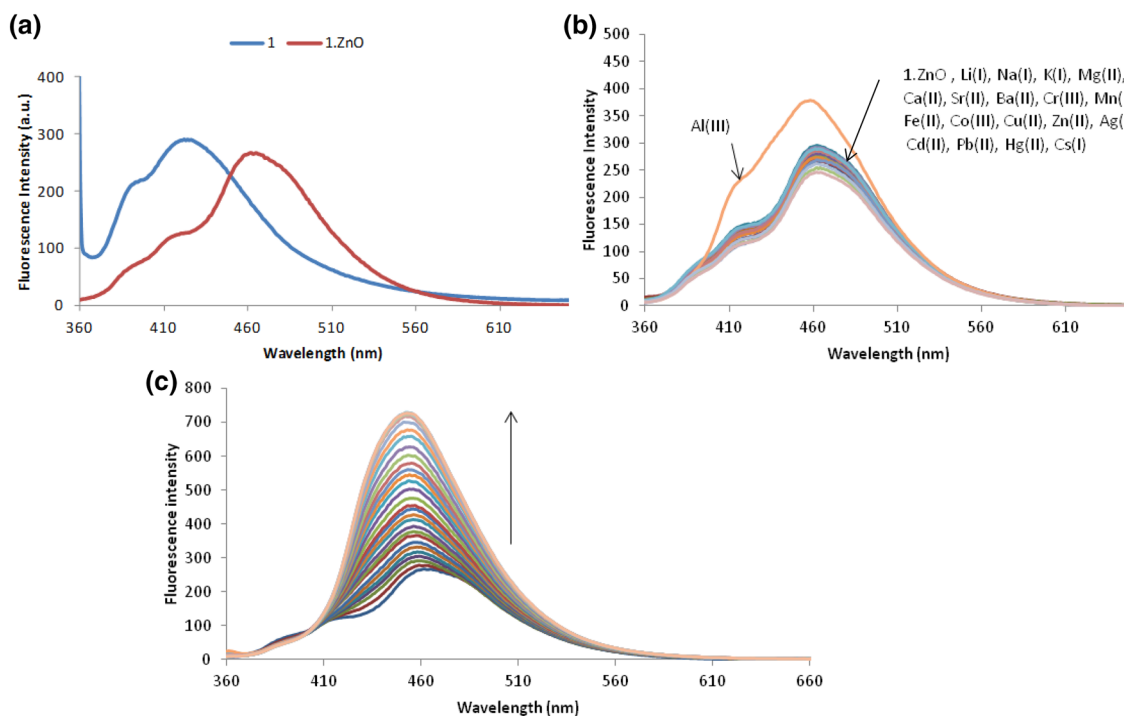


**Fig. 2** a Fluorescence emission spectra of **1.ZnO** nanoparticles ( $\lambda_{\text{ex}} = 341$  nm). b Changes in the fluorescence emission spectrum of 10  $\mu\text{M}$  solution of **1.ZnO** in DMSO:H<sub>2</sub>O (7:3 v/v) upon addition of

20  $\mu\text{M}$  of different metal ion salts ( $\lambda_{\text{ex}} = 341$  nm). c Changes in the fluorescence emission spectrum of **1.ZnO** upon successive addition of 0–100  $\mu\text{M}$  of  $\text{Al}^{3+}$  ( $\lambda_{\text{ex}} = 341$  nm)



binding test was carried out by mixing standard solutions of the sensor **1.ZnO** (10  $\mu\text{M}$ ) along with fixed amounts of a particular metal nitrate salt [20  $\mu\text{M}$  in HEPES-buffered in DMSO/ $\text{H}_2\text{O}$  (7:3, v/v)]. The changes in the PL spectra were recorded to monitor any change in the emission profile of **1.ZnO** in presence of the metal nitrate salts. The metal nitrate salts of different cations were added to the compound **1.ZnO** to study the effect. The emission spectra (centered at 461 nm) of **1.ZnO** has not shown any significant change with most of the metal ions tested, however the addition of  $\text{Al}^{3+}$  demonstrated enhancement in the fluorescence intensity in emission spectra. The increased fluorescence intensity caused by the addition of  $\text{Al}^{3+}$  cation in **1.ZnO** conjugate resulted in the increase in quantum yield and for the application of nanomaterials in the electronic device like LED, the quantum yield is a very important parameter to monitor. To observe further change in the emission spectra and thus the quantum yield, small aliquots of  $\text{Al}^{3+}$  were added and changes were observed using photoluminescence spectroscopy (Fig. 2c). The successive addition of  $\text{Al}^{3+}$  ion (0–100  $\mu\text{M}$ ) to the **1.ZnO** solution taken in 10 ml volumetric flask confirmed to the changes observed during the metal binding tests as an increase in the fluorescence intensity was observed upon addition of  $\text{Al}^{3+}$  ion. The fluorescence intensity has increased threefolds approximately upon binding of **1.ZnO** with  $\text{Al}^{3+}$  ions. The increase in the photoluminescence of ligand coated ZnO upon addition of Al(III) can be explained on the basis of PET phenomenon. Upon addition of Al(III), the lone pair of electrons available on Nitrogen atom of ligand bind with Al(III) (HSAB principle) which initially donated to fluorophore in the absence of Al(III), the fluorophore is now free to show fluorescence.

The receptor itself was checked for the metal binding studies with the metal nitrate salts but the ligand showed no selectivity for any of the metal ion (Fig. S5). The effect of pH on the fluorescence of **2** was also determined by fluorescence titration under different pH of solution from 2 to 11 and it was observed that **1.ZnO** can be safely used in the pH window 2–11 (Fig. S6). The influence of salt concentration was also checked by observing if any change has occurred in the emission spectra by adding perchlorate salt. The emission spectra remain intact even with addition of perchlorate salt (0–200  $\mu\text{M}$ ) which confirmed that the ionic strength up to 200  $\mu\text{M}$  has no effect on the **1.ZnO** nanoparticles (Fig. S7). The imine linked ZnO biocompatible nanoparticles functionalized with  $\text{Al}^{3+}$  ion can be used in electronic devices like LED as an improved quantum yield was observed. Also, ZnO being safe, biocompatible, non-toxic considering environmental issues can be picked for electronic devices. Thus, both pure and narrow line blue emission with enhanced quantum yield can be achieved with this proposed material. The introduced findings open a path

towards low cost, bio safe, lighting applications with excellent color selectivity.

## 4 Conclusion

ZnO semiconductor nanoparticles are very promising candidates for LED. Environmentally safe, biocompatible, stable alternative to conventional quantum dots utilized in existing LEDs is proposed as active light emitting material with both pure and narrow emission at 461 nm. The photophysical studies were carried out for organic receptor capped ZnO nanoparticles which established the emission at 461 nm. The photophysical studies were further investigated for **1.ZnO** in the presence of metal ions. The luminescent property of ZnO nanoparticles is optimized to achieve maximum quantum yield. Threefold improvements in the fluorescent intensity is achieved.

**Acknowledgements** CM acknowledges support from Dr. Renu Vig, Director, UIET for providing the lab facilities needed to carry out the research work. CM also acknowledges the SAIF department, Panjab University for the TEM, FTIR, Mass spectroscopy facilities provided and CNSNT department, Panjab University for sample nanofabrication facility and Photophysical studies. CM also acknowledges support from IIT Ropar, for providing DLS, SEM and EDX facility.

**Author contributions** The manuscript was written through contributions of all authors. All authors have given approval to the final version of the manuscript.

## Compliance with ethical standards

**Conflict of interest** The authors declare that they have no conflict of interest.

## References

1. R.J. Tseng, J. Ouyang, C.W. Chu, J. Huang, Y. Yang, *Appl. Phys. Lett.* **88**, 123506 (2006)
2. P. Uthirakumar, Y.S. Lee, E.K. Suh, C.H. Hong, *J. Lumin.* **128**, 287–296 (2008)
3. W.J.E. Beek, M.M. Wienk, R.A. Janssen, *J. Adv. Mater.* **16**, 1009–1013 (2004)
4. G. Fiori, F. Bonaccorso, G. Iannaccone, T. Palacios, D. Neumaier, A. Seabaugh, S.K. Banerjee, L. Colombo, *Nat. Nanotechnol.* **9**, 768–779 (2014)
5. D. Bera, L. Qian, T.K. Tseng, P.H. Holloway, *Materials* **3**, 2260–2345 (2010)
6. P.V. Kamat, *J. Phys. Chem. C* **112**(48), 18737–18753 (2008)
7. Y. Zhang, T.R. Nayak, H. Hong, W. Cai, *Curr. Mol. Med.* **13**(10), 1633–1645 (2013)
8. T.W. Prow, J.E. Grice, L.L. Lin, R. Faye, W. Butler, E.M.T. Wurm, C. Yoong, T.A. Robertson, H.P. Soyer, M.S. Roberts, *Adv. Drug Deliv. Rev.* **63**(6), 470–491 (2011)
9. A. Janotti, C.G. Van de Walle, *Rep. Prog. Phys.* **72**, 126501 (2012)
10. K. Okazaki, K. Kubo, T. Shimogaki, D. Nakamura, M. Higashihata, T. Okada, *Adv. Mater. Lett.* **2**(5), 354–357 (2011)

11. Q. Zhang, C.S. Dandeneau, X. Zhou, G. Cao, *Adv. Mater.* **21**, 4087–4108 (2009)
12. M.A. Abbasi, H.I. Zafar, H. Mushtaque, O. Nur, M. Willander, *Nanoscale Res. Lett.* **8**(320), 1–6 (2013)
13. N. Mandzy, E. Grulke, T. Druffel, *Powder Technol.* **160**, 121–126 (2005)
14. P.K. Giri, S. Bhattacharyya, B. Chetia, S. Kumari, D.K. Singh, P.K. Iyer, *J. Nanosci. Nanotechnol.* **11**, 1–6 (2011)
15. N. Goswami, D.K. Sharma, *Physica E* **42**(5), 1675–1682 (2010)
16. A.B. Lavand, Y.S. Malghe, *J. Saudi Chem. Soc.* **19**, 471–478 (2015)
17. Y. Cui, X. Shao, S. Prada, L. Giordano, G. Pacchiono, H.-J. Freund, N. Nilius, *Phys. Chem. Chem. Phys.* **16**, 12764 (2014)
18. R.M. Hewlett, M.A. McLachlan, *Adv. Mater.* **28**, 3893–3921 (2016)
19. A.M. Atta, H.A. Al-Lohedan, S.A. Al-Hussain, *Molecules* **19**, 11263–11278 (2014)
20. W. Wu, Q. He, C. Jiang, *Nanoscale Res. Lett.* **3**(11), 397–415 (2008)
21. K. Kobayashi, J. Wei, R. Iida, K. Ijiro, K. Niikura, *Polym. J.* **46**, 460–468 (2014)
22. K. Kim, H.B. Lee, J.W. Lee, H.K. Park, K.S. Shin, *Langmuir* **24**, 7178–7183 (2008)
23. U. Periyayya, J.H. Kang, J.H. Ryu, C.H. Hong, *Vacuum* **86**, 254–260 (2011)
24. C. Narula, I. Kaur, N. Kaur, *J. Mater. Sci.: Mater. Electron.* **26**, 791–800 (2015)
25. S. Kaur, A. Kaur, N. Kaur, *Mater. Lett.* **100**, 19–22 (2013)
26. H. Sharma, K. Narang, N. Singh, N. Kaur, *Mater. Lett.* **84**, 104–106 (2012)
27. C. Madhu, I. Kaur, N. Kaur, *J. Mater. Sci.: Mater. Electron.* **28**, 6388–6398 (2017)
28. H. Duan, D. Wang, Y. Li, *Chem. Soc. Rev.* **44**, 5778 (2015)
29. M. Rycenga, C.M. Cobley, J. Zeng, W. Li, C.H. Moran, Q. Zhang, D. Qin, Y. Xia, *Chem Rev.* **111**(6), 3669–3712 (2011)
30. H. Sharma, N. Kaur, T. Pandiyan, N. Singh, *Sens. Actuators B* **166–167**, 467–472 (2012)
31. S. Tongay, J. Suh, C. Ataca, W. Fan, A. Luce, J.S. Kang, J. Liu, C. Ko, R. Raghunathanan, J. Zhou, F. Ogletree, J. Li, J.C. Grossman, J. Wu, *Sci. Rep.* **3**, 2657 (2013). <https://doi.org/10.1038/srep02657>
32. S. Xu, Z.L. Wang, *Nano Res.* (2011). <https://doi.org/10.1007/s12274-011-0160-7>
33. W. Zhu, S. Kitamura, M. Boffelli, E. Marin, E.D. Gaspera, M. Sturaro, A. Martucci, G. Pezzotti, *Phys. Chem. Chem. Phys.* **18**, 9586 (2016)
34. A.-T.T. Do, H.T. Giang, T.T. Do, N.Q. Pham, G.T. Ho, *Beilstein J. Nanotechnol.* **5**, 1261–1267 (2014)
35. A.V. Dijken, E.A. Meulenkaamp, D. Vanmaekelbergh, A. Meijerink, *J. Phys. Chem. B* **104**, 1715–1723 (2000)
36. J.R. Sadaf, M.Q. Israr, S. Kishwar, O. Nur, M. Willander, *Nanoscale Res Lett.* **5**, 957–960 (2010)
37. S.B. Rana, A. Singh, N. Kaur, *J. Mater. Sci.: Mater. Electron.* **24**, 44–52 (2013)
38. A. Saini, J. Singh, R. Kaur, N. Singh, N. Kaur, *New J. Chem.* **38**, 4580–4586 (2014)